Imaging of the Aorta

6

Caroline A. Ball and Mark G. Rabbat

Imaging plays a significant role in diagnosis and management of diseases of the aorta. Over the past decade, technologic advances have expanded the ability to diagnose, monitor, and plan interventions for various disease states. We present a description of the utility of various modalities for imaging the aorta, as well as clinical implications.

Chest X-Ray

Chest x-ray was one of the first diagnostic modalities available for imaging of the aorta. It is a widely available, inexpensive modality, which can be obtained quickly at most centers. Findings on a PA chest x-ray that indicate aortic disease include a widened mediastinum or abnormal aortic contour. The left para-aortic interface can show increased convexity due to tortuosity of the thoracic descending aorta, aneurysm, or dissection [1]. However, the standard chest x-ray has limited utility for diagnosis, and more importantly exclusion, of aortic pathologies. Sensitivity of chest x-ray to identify acute aortic syndrome ranges from 64% to 71% [2]. Specificity of the chest x-ray for diagnosis of aortic dissection is 67%, 61% for non-dissecting aneurysm, and 63% for intramural hemorrhage or penetrating ulcer [3]. Sensitivity of the chest x-ray is lower for disease that is confined to the proximal aorta, than for disease in the distal aorta, likely due to obscuring of the image due to the cardiac silhouette [3]. Abnormalities identified on chest x-ray should be followed-up with additional imaging with higher sensitivity and specificity for aortic disease.

Imaging of the aortic arch may have other utility beyond diagnosing aortic disease. Calcification of the aortic arch on chest x-ray may play a role in prediction of cardiovascular events [4] and is related to calcification throughout the aorta [5], as well as coronary artery calcification [6].

Ultrasound

Ultrasound has many applications in the detection and monitoring of aortic disease. It has a variety of benefits, including its low cost, widespread availability, and the lack of radiation or IV contrast. Ultrasound is applied using several different techniques, each of which provides imaging of specific regions within the aorta.

Transthoracic Echocardiography

Echocardiography is a useful tool for diagnosing and monitoring a range of aortic diseases, particularly at the aortic root. Standard transthoracic echocardiography (TTE) uses several views, which allows visualization of the aorta in multiple locations.

Initial survey of the aorta occurs in the parasternal long axis on echocardiogram. To obtain this image, the transducer is placed at the third or fourth intercostal space, with the notch pointed toward the patient's right shoulder. The transducer may need to be displaced superiorly, such as to the second or third intercostal space, in order to obtain aortic measurements, particularly in patients with a dilated aorta [7, 8]. Moving the transducer closer to the sternum will bring a longer segment of the ascending aorta into view [8]. Measurements should be made perpendicular to blood flow. For the parasternal long axis view in patients with a tricuspid aortic valve, this can be achieved by aligning the closure line of the visualized leaflets in the center of the aortic root. This image allows for measurement of the sinus of Valsalva, the sinotubular junction, and the ascending aorta.

There is currently debate surrounding the landmarks for measuring diameter along the aorta in echocardiography.

C. A. Ball
Department of Medicine, Division of Cardiology, Loyola University Chicago, Maywood, IL, USA

M. G. Rabbat (✉)
Medicine and Radiology, Division of Cardiology, Loyola University Chicago, Maywood, IL, USA

R. S. Dieter et al. (eds.), *Diseases of the Aorta*, https://doi.org/10.1007/978-3-030-11322-3_6

Other imaging modalities, described below, have standardized measuring inner edge to inner edge. However, echocardiography has conventionally used leading edge to leading edge measurements. Reference values for aortic root measurements provided by the American Society for Echocardiography and the European Association of Cardiovascular Imaging are currently based on leading edge to leading edge measurements. It should be noted that using the inner edge to inner edge convention could modify measurements by 2–4 mm. Measurements should be obtained using 2D echocardiography, not M-Mode (Lange). Alternatively, the 2014 American College of Cardiology/American Heart Association (ACC/AHA) guidelines for diagnosis and management of thoracic aortic disease recommend measuring internal edge to internal edge [2].

The aortic root is measured in multiple locations on TTE, with reference values listed in Table 6.1 [8]. There are reference values available for measurement at the annulus, Sinuses of Valsalva, the sinotubular junction, and the ascending aorta. The Sinuses of Valsalva, the sinotubular junction, and the ascending aorta measurements should be obtained mid-diastole, and the widest diameter of the segment being measured should be used to evaluate for aortic dilatation. Aortic diameter should be indexed to a patient's body surface area [8, 9]. However, by convention, the aortic annulus is measured in peak systole, using the inner edge to inner edge [8].

A small cross-section of the descending aorta may be visualized in the parasternal long axis view, posterior to the left atrium. While there are no standard measurements available for this segment of the aorta, it should be visually inspected for abnormalities as part of a comprehensive TTE (Fig. 6.1).

In addition to the aortic root, TTE can be used to image the aortic arch using a view from the suprasternal notch. To obtain these images, the transducer should be placed above the patient's suprasternal notch, with the transducer indicator pointed to the patient's head. From this view, the three major supra-aortic vessels, the brachiocephalic, left common carotid, and left subclavian arteries, can be seen [7]. Velocities of blood flow through the aortic arch can be recorded using both continuous wave and pulse wave Doppler signals.

Table 6.1 Standardized aortic root measurements [8]

Aortic Root	Absolute values (cm)		Indexed values (cm/m^2)	
	Men	Women	Men	Women
Annulus	2.6 ± 0.3	2.3 ± 0.2	1.3 ± 0.1	1.3 ± 0.1
Sinus of Valsalva	3.4 ± 0.3	3.0 ± 0.3	1.7 ± 0.2	1.8 ± 0.2
Sinotubular junction	2.9 ± 0.3	2.6 ± 0.3	1.5 ± 0.2	1.5 ± 0.2
Proximal ascending aorta	3.0 ± 0.4	2.7 ± 0.4	1.5 ± 0.2	1.6 ± 0.3

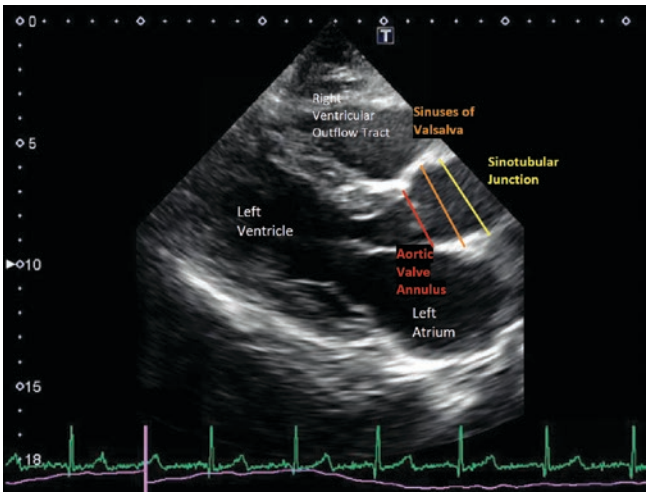

Fig. 6.1 Transthoracic echo, parasternal long axis view, diastole

Finally, portions of the abdominal aorta may be seen from the subcostal view to the left of the inferior vena cava. There are no society-recommended guidelines for imaging the abdominal aorta from this view, but abnormalities identified on this TTE view can prompt further diagnostic studies for imaging of the entire aorta.

Dilation of any one segment of the aorta as identified on TTE should prompt further imaging of the entire aorta. Measurements should be considered in the context of the patient's sex and indexed to the patient's body surface area.

TTE has additional diagnostic value for identifying and following disease processes of the aorta. First, echocardiography provides significant structural and functional information about the patient's heart, which may contribute to their aortic pathology. For example, TTE can identify a bicuspid aortic valve, which may be associated with an aortopathy.

TTE has particular utility for diagnosing and monitoring dilatation and aneurysm of the aortic root, with the benefit of being a noninvasive, relatively low-cost test without the need for radiation or contrast. Sinus of Valsalva aneurysms are a unique group of aneurysms of the aortic root that can be identified and followed on TTE. These aneurysms frequently arise from the right coronary sinus and project into the right atrium, causing the "windsock deformity." Alternatively, a sinus of Valsalva aneurysm that arises from the non-coronary cusp may be seen projecting into the interventricular septum (Fig. 6.2).

TTE can identify acute aortic dissection, although this is limited primarily to dissections of the aortic root. TTE has a sensitivity of 78–90% for identifying ascending aortic dissection, but a 31–55% sensitivity for identifying descending aortic dissection. TTE has a specificity of 87–96% for Type A aortic dissections, with a lower specificity for Type B

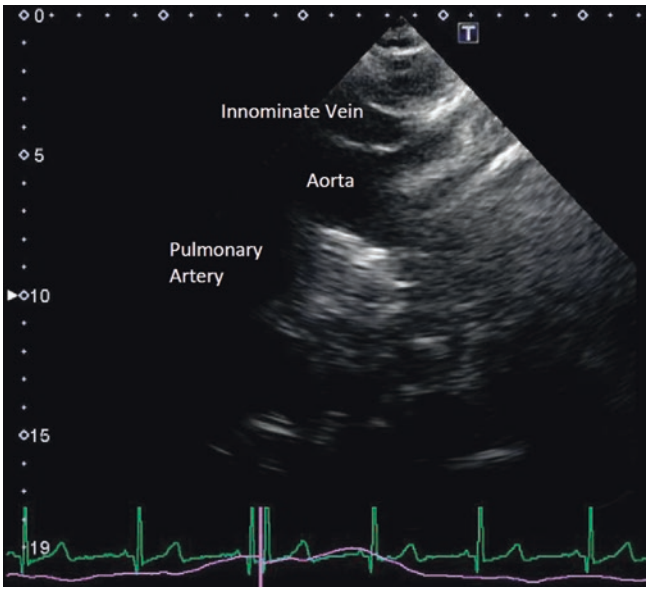

Fig. 6.2 Transthoracic echo, suprasternal notch view

aortic dissections, from 60% to 83%. The sensitivity can be improved by using ultrasound contrast agents [9]. Given its inability to visualize the entire aorta and its inferior sensitivity to other modalities listed later, TTE should not be used as the initial test to rule out aortic dissection.

Diagnosis of dissection requires identifying both a true and false lumen, including the dissection flap. The dissection flap should have motion that is independent of its surrounding structures. This flap should be contained within the lumen of the aorta. Differentiating between the true and false lumens can be challenging on 2D echocardiography, but there are several features that echocardiographers can use to identify the true and false lumen. The true lumen should expand during systole and contract during diastole. In calcified vessels, the true lumen may have surrounding calcification and have a more regular shape than the false lumen. There should be little or no spontaneous echo contrast through the true lumen, and the systolic jets should direct away from the transducer when color flow is studied through the vessel. Often, the false lumen has a wider diameter than the true lumen and may contain strand-like structures, which are referred to as "cobwebs." The false lumen may have spontaneous echo contrast or thrombus and is often bigger than the true lumen [7, 10].

After identification of aortic dissection, TTE can be used to identify complications of the dissection, such as pericardial effusion, aortic regurgitation, and wall motion abnormalities caused by dissection through the coronary ostia.

Continuous wave Doppler through the aortic arch on the suprasternal notch view can be used to identify coarctation of the aorta. There should be increased velocities across the area of coarctation, although this requires accurate Doppler signals [7, 11]. Similarly, a persistent ductus arteriosus can be identified using color Doppler [9].

Although TTE should not be used for imaging of the entire aorta, it is useful for follow-up imaging of dilatation of the aortic root, particularly in patients who will require many serial measurements [2, 9].

Transesophageal Echocardiography

Transesophageal echocardiography (TEE) was initially developed to measure flow in the aortic arch and has remained an important modality for imaging the aorta since its inception. TEE provides an additional modality for imaging the aorta without the need for radiation or iodinated contrast exposure. TEE is a more invasive test than TTE, but has several advantages, including permitting visualization of the majority of the aorta. Similar to TTE, the aorta can be visualized in multiple views on TEE. The American Society of Echocardiography describes 28 specific views for obtaining a TEE [12]. Below, we will describe those that are relevant to imaging the aorta.

The aortic root is best visualized on TEE using the midesophageal aortic valve long-axis view and the midesophageal ascending aorta long axis view [8, 12]. The midesophageal aortic valve short axis and transgastric views can be helpful for imaging the aortic valve. The midesophageal aortic valve long axis view is obtained by inserting the transducer to the midesophagus with the transducer angle at 120–140°. From this view, the midesophageal ascending aorta long axis view can be obtained by withdrawing the probe to the upper esophagus and adjusting the transducer angle to 90–110°. The midesophageal ascending aortic short and long axis views are important for excluding aortic dissection [13] (Fig. 6.3).

A significant portion of the descending aorta can be visualized using TEE. To obtain images beginning at the upper abdominal aorta, the transducer should be inserted to the transgastric view until the aorta is no longer in view. This is around the location of the celiac trunk. Subsequently, the transducer is slowly withdrawn, allowing careful inspection of the aortic lumen. Using simultaneous multiplane imaging, the aorta can be seen in both the descending aortic long and short axis views. The probe is withdrawn to the level of the left subclavian artery, forming the upper esophageal aortic arch long and short axis views. By rotating the transducer angle from 0° (upper esophageal aortic arch long axis view) to 90–110° (upper esophageal aortic arch short axis view), the arch and descending aorta can be seen in multiple views. Additionally, from the upper esophageal aortic arch short axis view a patent ductus arteriosus or coarctation of the aorta can be identified. Other views that can be useful for imaging the aorta include the midesophageal ascending short axis and the upper esophageal aortic arch long and short axes.

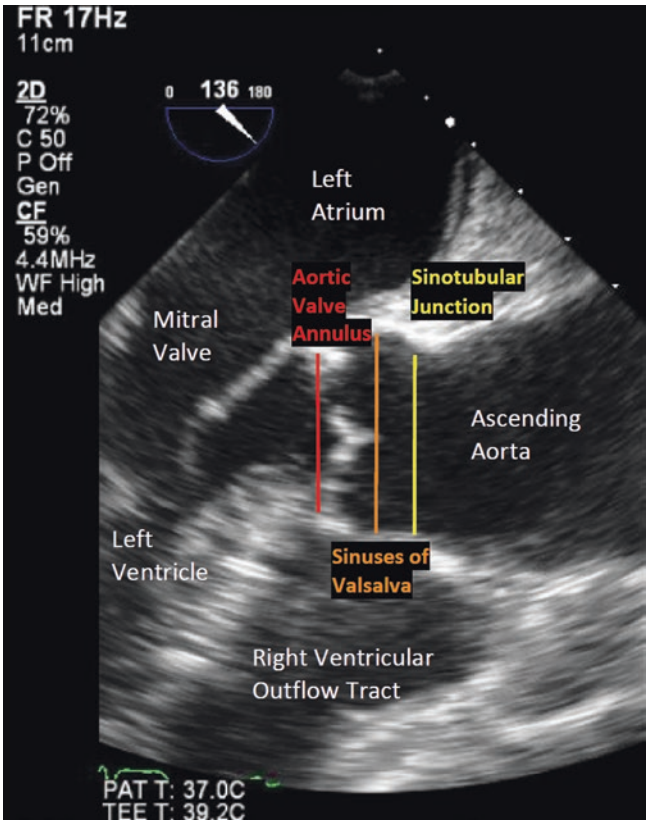

Fig. 6.3 Transesophageal echocardiogram, midesophageal aortic valve long axis view

TEE evaluation of the aorta is limited by a "blind spot" in the aortic arch, where the trachea is interposed between the esophagus and the aortic arch, causing air artifact and limiting visualization of the arch. This is of particular importance in surgery requiring cardiopulmonary bypass, as cannulation occurs in an area of the ascending aorta that may not be adequately visualized. In some situations, this "blind spot" can be overcome with the use of a fluid-filled catheter, which is referred to as an "A-View." This technique involves placing a fluid-filled intratracheal balloon down the left main stem bronchus in intubated patients to create an echo window for imaging of the aortic arch [14].

The American Society of Echocardiography recommends measuring the aortic root on TEE at several locations, including the aortic valve annulus, designated by the hinge points of the aortic leaflets, the maximal diameter in the sinus of Valsalva, and the sinotubular junction. Similar to TTE, there is no consensus on the ideal technique for measuring the aorta, but normative standards are provided for adults using the leading edge to leading edge technique. Measurements should be made using 2D echocardiography, not M-Mode [12]. Normal measurements of the aortic root are similar between TTE and TEE, and the reader is directed to Table 6.1 for standard aortic root measurements on TEE. TEE can also be used to measure the aortic arch and the descending aorta. However, TEE measurements of the descending aorta are prone to error if oblique measurements are made. Therefore, measurements should only be recorded if the aorta is visualized with circular cross-sections. Standard measurements of the descending aorta are not indexed to body surface area. Standard diameter of the aortic arch is measured proximal to the innominate artery and is 22–36 mm. Standard diameter of the descending aorta is obtained between the ligamentum arteriosum and the diaphragm and is 20–30 mm.

The American Society of Echocardiography encourages documenting any irregularities of the aortic wall, in addition to the presence and thickness of atheroma and the presence of mobile atherosclerotic elements. Locations of aortic findings should be documented relative to the left subclavian artery or relative to the incisors.

Color Doppler can be used to evaluate for abnormal flow in the thoracic aorta, particularly in the setting of atheroma or a known dissection flap. Although an emerging technique, 3D TEE has potential to improve measurements obtained by TEE.

TEE has the ability to identify atherosclerotic plaques in the aorta, which can be of particular interest in patients undergoing surgery requiring cardiopulmonary bypass. Atherosclerotic plaques appear as a thickness within the aortic wall. Whenever they are identified, they should be described with respect to their thickness and the presence of any mobile components. Several scoring systems have been implemented to better describe the stroke risk associated with each plaque. Perhaps the most widely accepted is the Katz score, which is described in Table 6.2 [15].

Based on a recent meta-analysis, standard TEE itself has limited sensitivity for aortic atherosclerosis, as low as 21%, but high specificity, up to 99% [14]. Thus, it is frequently used in conjunction with other aortic imaging techniques, such as epiaortic scanning or the A-view technique described above to identify aortic atherosclerosis. TEE can be used to identify aortic aneurysms, as well as to describe the size, location, and extent of the aneurysm, and the presence of a hematoma within the aneurysm. Whereas TEE has limited sensitivity for atherosclerosis, its sensitivity for aortic dissection is high (86–100%) and its specificity is high (90–100%) [16]. TEE is limited in its evaluation of aortic dissection by its difficulty in assessing the distal ascending aorta and the proximal aortic arch [13]. In patients with dissection, similar techniques can be used in TEE as were described for TTE for distinguishing between the true and false lumens.

Table 6.2 The Katz score for describing aortic atherosclerosis [15]

Grade	Description
I	Normal to mild intimal thickening
II	Severe intimal thickening without protruding atheroma
III	Atheroma protruding 3 to 5 mm into the lumen
IV	Atheroma protruding >5 mm into the lumen
V	Any thickness with mobile component

Abdominal Ultrasound

Abdominal aortic ultrasound is another noninvasive and inexpensive tool for imaging the aorta. Abdominal aortic ultrasound allows visualization of the abdominal aorta from the diaphragm to the bifurcation of the aorta [11]. Images are obtained using a 2.5–5.0 MHz curvilinear array transducer. The patient is placed either in the supine or left lateral decubitus position and encouraged to fast for 8–12 hours prior to the procedure to reduce intestinal gas. The abdominal aorta should be imaged in both the longitudinal and transverse planes along the entire distance from the diaphragm to the bifurcation. Measurements should be obtained in the most circular cross-sectional image possible, measured in the anterior-posterior diameter from outer edge to outer edge. Inter-observer reproducibility for measuring the abdominal aorta is ± 1.9 mm to ± 10.5 mm [11].

One of the foremost uses of abdominal ultrasound is for screening of abdominal aortic aneurysms (AAA). Abdominal ultrasound has a sensitivity of 94–100% for detecting AAA and a specificity of 98–100% [17]. Between 1988 and 1999, four major randomized controlled trials (RCT) examined screening programs for AAA. Meta-analysis of these four trials found that screening programs reduced AAA mortality by 40% after 3–5 years and a 2.7% reduction in all-cause mortality at 11–15 years follow-up [18, 19]. Each of these RCTs used a 30 mm infrarenal diameter as a cutoff for diagnosis of AAA, with surgical repair recommended for an infrarenal abdominal aortic diameter greater than 5.5 cm in men and 5.0 cm in women. However, the protocols within the RCTs used differing techniques for measurement of the AAA, including inner edge to inner edge, leading edge to leading edge, and outer edge to outer edge. The United States Preventive Services Task Force recommends a one-time ultrasonography screening for AAA in men aged 65–75 years who have ever smoked. This recommendation does not specify how the abdominal aortic diameter should be measured (Fig. 6.4).

Contrast agents are now available to enhance ultrasound images. Ultrasound contrast agents use microbubbles that reflect non-linear signals, enhancing the definition of tissue lines. Contrast agents have been used in abdominal ultrasound for enhanced imaging of AAA and for better visualizing aortic rupture [20]. Following endovascular aortic aneurysm repair, abdominal ultrasound can be used to visualize endoleaks, fractures, or progressive enlargement of an AAA as part of a surveillance program. Contrast-enhanced ultrasound is the imaging modality of choice for following these patients, as it does not require radiation, it is fast and affordable, and it has high sensitivity and specificity for diagnosing endoleaks, 98–100% and 82–93%, respectively [20].

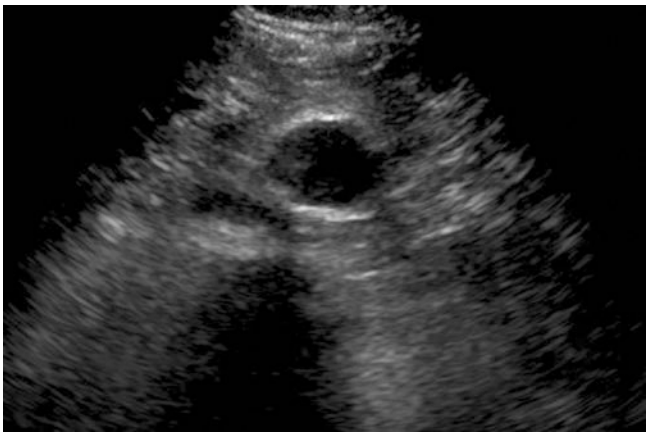

Fig. 6.4 Ultrasound of the abdominal aorta with an infrarenal aneurysm

Epiaortic Scanning

Aortic atherosclerosis is a significant risk factor for post-cardiac surgery stroke, and its identification prior to a surgical procedure can assist surgeons in forming a surgical plan. Epiaortic scanning (EAS) uses a high-frequency, linear array transducer to image the ascending aorta and the aortic arch prior to surgical manipulation of the aorta. Epiaortic scanning has the advantages of being able to image the entire aorta [21], and its use changes surgical plans 4–31% of the time, potentially reducing the risk of perioperative stroke [22]. However, epiaortic screening cannot be performed until after the sternotomy has been completed, leaving a surgeon limited time to adjust surgical planning. Additionally, introducing the ultrasound transducer to the surgical field increases risk of infection and complication. Prior to the introduction of A-view technique for TEE, epiaortic scanning was one of few methods surgeons had for visualizing aortic plaque without direct palpation of the aorta. A-view technique now allows surgeons to visualize the entire aorta prior to sternotomy.

Intravascular Ultrasound

A new area of ultrasound evaluation of the aorta is using intravascular ultrasound (IVUS). This technique involves introducing a catheter with an ultrasound probe into the patient's arterial system, most commonly through the femoral artery. The probe is inserted into the left ventricle and then slowly withdrawn to the desired level, with measurements of aortic diameter obtained along the way. This invasive approach may be of interest in the setting of transcatheter aortic valve implantation, as it provides accurate measurements of the lumen where the valve is to be implanted. Early studies demonstrate consistent aortic annular measurements obtained using IVUS and those using computed tomography (CT)

[23]. However, the correlation may be less robust in the aortic arch, where IVUS tends to measure a larger diameter compared to CT [24]. IVUS may have additional benefits in measuring variation of aortic diameter over the cardiac cycle [25].

At the time of writing, there are no specific reference standards for aortic measurements obtained by IVUS, but the reader may refer to reference standards provided for CT.

Computed Tomography

CT provides a wealth of information about the aorta. It has many advantages over other modalities, including its ability to image the entire aorta, visualizing the lumen, wall, and periaortic regions. CT can rapidly acquire high-quality images, allowing prompt diagnosis of acute aortic syndromes. Best practice CT imaging of the aorta uses ECG-gating to reduce artifact from cardiac motion, by synchronizing image acquisition to the cardiac cycle. Specifics of ECG gating are beyond the scope of this discussion [2]. CT angiography (CTA) uses iodinated contrast agents to permit improved delineation of the aorta and additional blood vessels.

Individual institutions have specific protocols for obtaining CT images of the aorta. The ACC/AHA recommend using at least four detector rows to image the thoracic aorta, with ≥3 mm thickness and a reconstruction level of 50% or less than the slice thickness with ≤50% overlap [2].

In general, imaging protocols should begin with a non-contrast image to identify the subtle changes associated with intramural hematoma, which may not be identified on contrast enhanced imaging. Next, contrast media can be introduced for improved delineation of the aortic lumen. If given, it should be injected at 3–5 mL/second via a power injector, with a total volume delivered ≤150 mL. Contrast material should be injected into the right upper extremity, as contrast delivered through the left brachiocephalic vein can result in streaking. Contrast administration is particularly important for identifying dissection flaps [2]. Imaging should extend from above the aortic arch to at least the aortoiliac bifurcation for a comprehensive aortic examination. In the setting of dissection, a field from the aortic arch to the aortoiliac bifurcation allows inspection of aortic branch vessels for malperfusion and involvement in dissection, as well as allows planning for an endovascular repair. Delayed images should be used when evaluating patients after stent-graft repair of aortic aneurysms to detect endoleaks [26]. For patients with an endoleak identified on CTA, additional imaging should be obtained with digital subtraction angiography.

Measurements obtained with CT should be performed relative to the centerline of flow to ensure that measurement occurs at a true short axis, perpendicular to the line of blood flow. More recently, the use of 3D reconstructions has allowed improved interpretation of axial section [2]. The convention in CT is to measure outer edge to outer edge. This can result in a significant discrepancy between measured aortic diameter and actual aortic lumen in the setting of intraluminal clot, aortic wall inflammation, or aortic dissection, as well as a discrepancy between measurements obtained on CT and using echocardiography (Fig. 6.5).

Due to the differences in imaging technique, there are a unique set of reference aortic diameters for CT than for echocardiography. Measurements are considered relative to the patient's age and sex. Each patient's specific measurements must be placed in the context of their clinical condition, as criteria for intervention of aortic aneurysm may be specific to disease process, such as in genetic aortopathies. Measurements should be normalized to body surface area. Reference values for aortic area as measured by CT are listed in Table 6.3 [27].

Inter-observer variability for CT evaluation of AAA is approximately 5 mm, and intra-observer variability is approximately 3 mm [11].

Imaging reports, regardless of modality used, should include several important elements, as recommended by the ACC and the AHA [2]. These elements include:

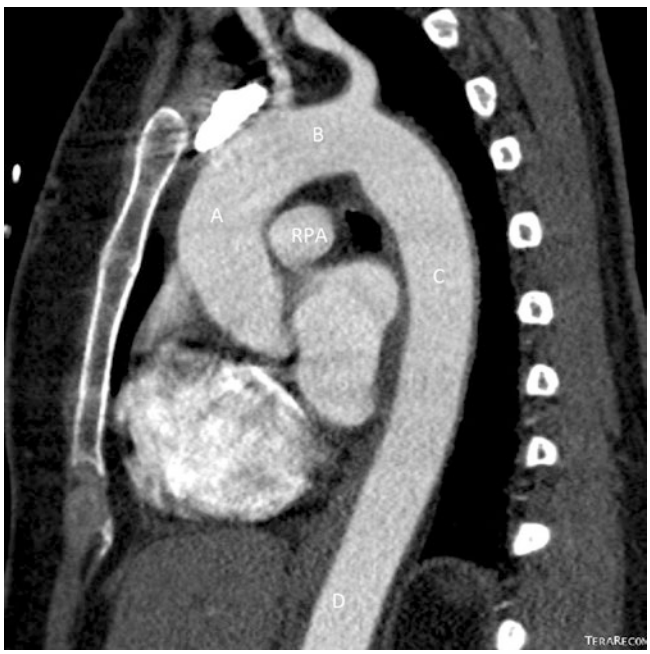

Fig. 6.5 CT image, lateral projection of the thoracic aorta. Legend: A = ascending aorta. B = aortic arch. C = thoracic descending aorta. D = abdominal descending aorta. RPA = right pulmonary artery

Table 6.3 Reference values for aortic diameter on CT [27]

	Ascending aorta		Descending aorta	
Age (years)	Male	Female	Male	Female
<45	3.9 ± 0.8	3.8 ± 0.7	2.0 ± 0.3	2.1 ± 0.3
45–54	4.4 ± 0.8	4.3 ± 0.8	2.2 ± 0.3	2.4 ± 0.4
55–64	4.7 ± 0.9	4.7 ± 0.9	2.4 ± 0.4	2.6 ± 0.4
≥65	5.2 ± 0.9	5.1 ± 0.9	2.7 ± 0.4	2.7 ± 0.4

Units are cm^2/m^2

1. The location at which the aorta is abnormal.
2. The maximum diameter of any dilatation, measured from the external wall of the aorta, perpendicular to the axis of flow, and the length of the aorta that is abnormal.
3. For patients with presumed or documented genetic syndromes at risk for aortic root disease measurements of the aortic valve, sinuses of Valsalva, sinotubular junction, and ascending aorta.
4. The presence of internal filling defects consistent with thrombus or atheroma.
5. The presence of intramural hematoma, penetrating aortic ulcer, and calcification.
6. Extension of aortic abnormality into branch vessels, including dissection and aneurysm, and secondary evidence of end-organ injury.
7. Evidence of aortic rupture, including periaortic and mediastinal hematoma, pericardial and pleural fluid, and contrast extravasation from the aortic lumen.
8. When a prior examination is available, direct image to image comparison to determine if there has been any increase in diameter.

One of the significant advantages of CT over previously described imaging modalities for the aorta is its high sensitivity and specificity. CT has a sensitivity as high as 100% and a specificity as high as 100% for diagnosis of aortic dissection [16] and a sensitivity of 90% and a specificity of 91% for AAA [17].

Due to the rapid acquisition of CT images, this modality is particularly beneficial in the trauma setting. For trauma patients, the sensitivity, specificity, and accuracy of contrast-enhanced multidetector CT for traumatic injuries are 96%, 99%, and 99%, and the negative predictive value of a non-contrast CT of the aorta approaches 100% [2]. Additionally, CT is favored over MRI for imaging of the aorta after an intervention or open surgery due to the presence of metallic closure devices and clips.

CT plays an important role in the diagnosis and management of aortic dissection, particularly with identification of the true and false lumens and the site of intimal tear. According to the International Registry of Acute Aortic Dissection, CT is the initial modality for diagnosis of aortic dissection in 61% of cases [2]. Similar to echocardiography, there are several techniques that can be used to differentiate the true from the false lumen. In highly calcified aortas, the true lumen may retain an intraluminal ring of calcification. The true lumen is generally smaller than the false lumen and will be continuous with the remainder of the aorta. "Cobwebs," linear low attenuation areas within the false lumen, are highly specific for identifying the false lumen. Thrombi may be seen in the false lumen, as well as the "beak sign," which indicates the area of intimal tear [28] (Fig. 6.6).

CT can be used to identify several specific disease conditions. Aortic rupture can be identified on CT, although the clinical situation rarely allows time for thorough examination. Aortic rupture often appears as a periaortic hematoma on a

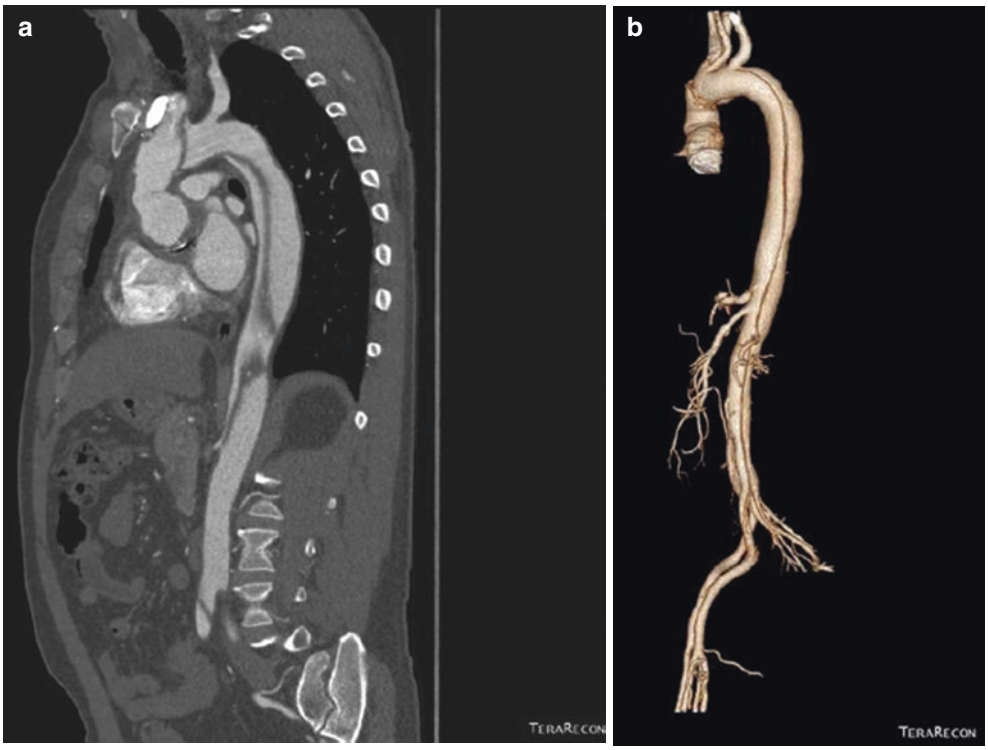

Fig. 6.6 (**a**) CT image, lateral projection of the thoracic and abdominal aorta with a large aortic dissection. (**b**) 3D reconstruction images from CT of the thoracic and abdominal aorta, with a large aortic dissection

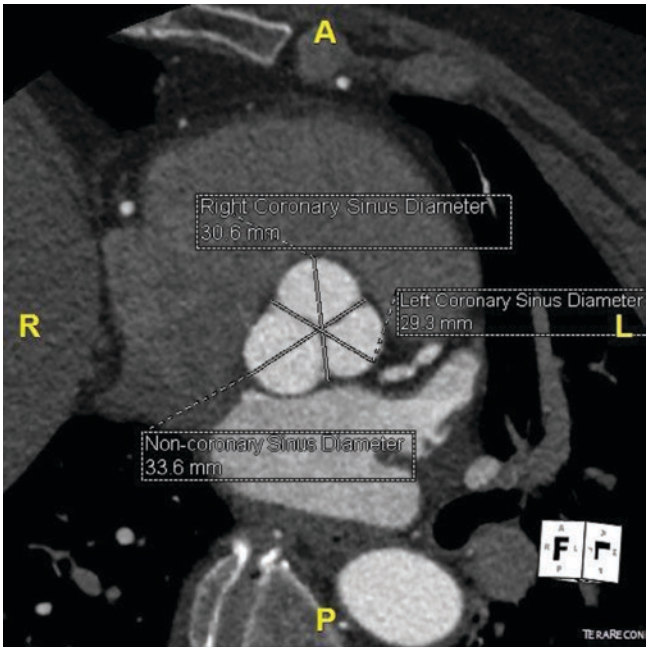

Fig. 6.7 Sinus of Valsalva diameter on CT

non-contrast image or is demonstrated by contrast extravasation into the pleura, mediastinum, or retroperitoneum. Prior to rupture, CT can identify areas of vascular instability. The "hyperattenuating crescent sign" is a high density within an aneurysm and is best seen on non-contrast studies. This represents fresh hemorrhage mixed with established mural clot. Additionally, diminishing internal thrombus may suggest dynamic vessel walls. Mycotic aneurysms can be seen on CT. Mycotic aneurysms appear saccular, with a wide neck, eccentric or multilobulated periaortic inflammation, and/or with air. Inflammatory aneurysms, more frequently seen in the abdominal aorta, present as a soft tissue ring around the aorta on cross-sectional imaging. They may be accompanied by soft tissue thickening that adhered to adjacent retroperitoneal structures, leading to loss of periaortic fat planes or medial deviation of the ureters. Penetrating aortic ulcer usually presents as an irregular, "crater-like" contrast-filled outpouching extending beyond the aortic lumen. Aortitis may present as increased wall thickening, and individual disease processes can be difficult to differentiate on CT. Giant cell arteritis tends to involve the thoracic aorta and may present with "skip lesions," whereas Takaysu's arteritis more commonly affects the left subclavian artery or the abdominal aorta [28] (Fig. 6.7).

Magnetic Resonance Imaging

Magnetic resonance imaging (MRI) provides a complete image of the aorta with excellent anatomical detail. With the proper sequences, MRI has the additional benefit of providing functional imaging, including aortic valve and left ventricular function analysis. However, MRI is not readily available at all centers, and imaging techniques can take 2–4 times longer compared to a CT acquisition. Additionally, MRI requires patients to remain still in a confined space for a prolonged period, which limits its utility for patients with claustrophobia. Due to the use of magnets in image acquisition, MRI cannot be used on patients with certain metal implants [2].

While specifics of MRI are beyond the scope of this text, the reader should be aware that there are several different types of pulse sequences, combinations of radiofrequency pulses, and magnetic gradients that are used to acquire an image. Specific pulse sequences provide optimal imaging for different components of the aorta and various disease processes [29].

Protocols for obtaining MR images are specific to institutions. In general, imaging should begin with spin-echo black blood sequences to outline the shape and diameter of the aorta. Spin-echo black blood sequences also permit detection of an intimal flap in the setting of an aortic dissection. Next, gradient-echo bright blood sequences can be used to demonstrate changes in the aortic diameters throughout the cardiac cycle, as well as to detect any blood flow turbulence. Gadolinium contrast agents can be used to better delineate the vessel wall [1]. When contrast agents cannot be used, ECG-gated non-contrast steady state free precision images can be used to obtain aortic diameter [11, 30]. Source and maximal intensity projection images can be evaluated for delineation of the aortic wall and for imaging of the dissecting membrane. Time-resolved 3D flow-sensitive MRI allows visualization and measurement of blood flow patterns and shear wall stress [11]. Additionally, maximum intensity projection imaging allows visualization of collateral circulation [28]. Aortic wall inflammation can be identified using T2-weighted images by evaluating for wall edema, or by post-contrast wall enhancement [30] (Fig. 6.8).

MRI can be used to measure vessel diameter throughout the aorta. Measurements should be obtained at similar locations along the aorta as described above for CT and should be obtained perpendicular to the axis of blood flow, at the widest point of the vessel [2]. ECG gating should be used to minimize motion artifact [1]. Measurements should use the outer edge-to-outer edge technique, although this continues to be a topic for debate [31]. There are fewer published normal aortic diameter values for MRI than for other modalities. However, normal values, as obtained by Davis et al., are listed in Tables 6.4 and 6.5. Measurements should be compared to normal values for age and sex, as the aortic lumen diameter, total vessel diameter, and wall area normally increase with age [30, 32].

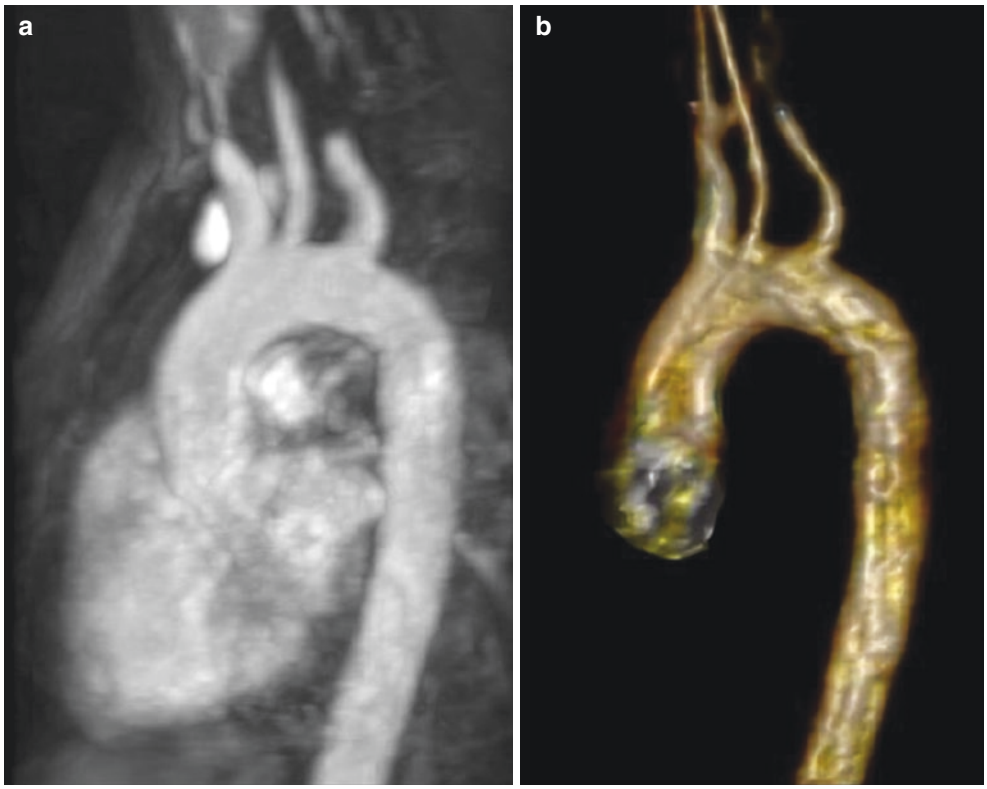

Fig. 6.8 (**a**) MR image, maximum intensity projection of the thoracic aorta. (**b**) MRI 3D reconstruction of the thoracic aorta

Table 6.4 Normal values (in mm) of the thoracic and abdominal aortic luminal diameters for men and women of different BMI categories measured on MRI at diastole [31]

	Men			Women		
BMI (kg/m²)	<25	25–29.9	>30	<25	25–29.9	>30
Aortic annulus	23.9 (18.6–29.2)	24.3 (18.9–29.7)	25.6 (20.4–30.8)	20.6 (17.4–23.8)	21.7 (18.4–25.0)	21.5 (17.2–25.8)
Aortic sinus	31.9 (24.3–39.5)	32.8 (25.2–40.4)	33.3 (24.3–42.3)	27.5 (21.9–34.2)	28.0 (21.8–34.2)	27.5 (21.3–33.7)
Sinotubular junction	24.4 (18.2–30.6)	25.7 (16.7–34.7)	26.2 (18.9–33.5)	21.6 (16.6–26.6)	22.3 (17.0–27.6)	22.1 (15.9–28.3)
Ascending aorta	26.0 (18.7–33.3)	27.4 (18.9–35.9)	28.5 (23.1–33.9)	24.7 (17.8–31.6)	26.5 (19.3–33.7)	26.6 (18.8–34.4)
Proximal descending aorta	20.1 (14.7–25.5)	20.9 (15.6–26.2)	22.2 (16.3–28.1)	18.5 (14.6–22.4)	19.2 (14.8–23.6)	19.6 (16.5–23.2)
Abdominal aorta	17.1 (12.0–22.2)	17.9 (12.8–23.0)	18.8 (14.4–23.2)	16.0 (12.1–19.9)	16.3 (12.3–20.3)	17.4 (13.9–20.9)

Values are given as (Mean [±2 SD])
BMI Body mass index

Table 6.5 Absolute and BSA-indexed normal values of ascending aortic luminal diameter for men and women of different age categories measured on MRI phase contrast images [31]

Age (years)	Men	Women
Absolute values (mm)		
45–54	31.6 (27.2–37.3)	28.8 (24.6–34.4)
55–64	32.8 (28.1–40.7)	30.1 (25.7–36.4)
65–74	34.2 (28.7–41.0)	30.6 (26.1–36.3)
75–84	34.7 (28.6–40.8)	31.1 (26.8–37.1)
Values indexed to BSA (mm/m²)		
45–54	15.9 (13.3–19.5)	16.7 (13.5–20.7)
55–64	16.8 (13.6–21.1)	17.6 (14.4–22.1)
65–74	17.8 (14.2–21.8)	18.1 (14.5–22.1)
75–84	18.6 (15.2–22.6)	19.7 (15.3–28.2)

Values are given as (Median [5th–95th percentile])
BSA Body surface area

Major society guidelines recommend MRI for repeat imaging of the aorta, particularly for any location distal to the aortic root to minimize radiation to the patient and optimize reproducibility [2].

MRI has a 95–100% sensitivity and 94–98% specificity for diagnosing aortic dissection [16]. MRI allows specific characterization of aortic atheroma with visualization of the fibrous cap, lipid core, and thrombus [22] (Fig. 6.9).

Fig. 6.9 Thoracic magnetic resonance angiogram, maximum intensity projection of the thoracic aorta demonstrating coarctation of the aorta (white arrow)

Conclusion

Significant advances in imaging techniques over the past decade have expanded the ability to noninvasively diagnose, monitor, and plan interventions for a variety of aortic pathologies. While established imaging techniques such as TTE and TEE continue to play an important role in imaging of the aorta, highly sensitive and specific modalities such as CT and MRI are playing an expanding role and are invaluable tools for the diagnosis and management of aortic diseases.

Acknowledgment The authors thank Vasilios Vasilopoulos, AA, AAS, R.T.(R) (3D Technologist, Radiology, Loyola Medical Center) for assistance with image formatting and 3D reconstruction.

References

1. Mongeon F, Marcotte F, Terrone DG. Multimodality noninvasive imaging of thoracic aortic aneurysms: time to standardize? Can J Cardiol. 2016;32(1):48–50.
2. Hiratzka LF, Bakris GL, Beckman JA, et al. 2010 ACCF/AHA/AATS/ACR/ASA/SCA/SCAI/SIR/STS/SVM guidelines for the diagnosis and management of patients with thoracic aortic disease. J Am Coll Cardiol. 2010;55(14):e27–129.
3. Von Kodolitsch Y, Nienaber CA, Dieckmann C, Schwartz AG, et al. Chest radiography for the diagnosis of acute aortic syndrome. Am J Med. 2004;116(2):73–7.
4. Iiijima K, Hashimoto H, Hashimoto M, et al. Aortic Arch calcification detectable on chest x-ray is a strong independent predictor of cardiovascular events beyond traditional risk factors. Atherosclerosis. 2010;210(1):137–44.
5. Hashimoto H, Iijima K, Hashimoto M, Son BK, Ota H, Ogawa S, Eto M, Akishita M, Ouchi Y. Validity and usefulness of aortic arch calcification in chest X-ray. J Atheroscler Thromb. 2009;16(3):256–64.
6. Bannas P, Jung C, Blanke P, Treszl A, Derlin T, Adam G, Bley TA. Severe aortic arch calcification depicted on chest radiography strongly suggests coronary artery calcification. Eur J Radiol. 2013;23(10):2652–7.
7. Quader N, editor. The Washington manual of echocardiography. 2nd ed. Philadelphia: Wolters Kluwer; 2017.
8. Lang RM, et al. Recommendations for cardiac chamber quantification by echocardiography in adults: an update from the American Society of Echocardiography and the European Association of Cardiovascular Imaging. J Am Soc Echocardiogr. 2015;28(1):1–39.e14.
9. Evangelista A, Flachskampf F, Erbel R, et al. Echocardiography in aortic diseases: EAE recommendations for clinical practice. Eur J Echocardiogr. 2010;11:645–58.
10. Oh JK, Seward JB, Tajik AJ, editors. The Echo manual. 3rd ed. Philadelphia: Lippincott Williams & Wilkins; 2012.
11. Erbel R, Aboyans V, Boileua C, et al. The task force for the diagnosis and treatment of aortic diseases of the European Society of Cardiology. 2014 ESC guidelines on the diagnosis and treatment of aortic diseases. Eur Heart J. 2014;35:2873–926.
12. Hahn RT, et al. Guidelines for performing a comprehensive transesophageal echocardiographic examination: recommendations from the American Society of Echocardiography and the Society of Cardiovascular Anesthesiologists. J Am Soc Echocardiogr. 2013;26:921–64.
13. Patil TA, Nierich A. Transesophageal echocardiography evaluation of the thoracic aorta. Ann Card Anaesth. 2016;19(Supplement):S44–55.
14. Van Zaane B, Nierich AP, Buhre WF, Brandon Bravo Bruinsma GJ, Moons KG. Resolving the blind spot of transesophageal echocardiography: a new diagnostic device for visualizing the ascending aorta in cardiac surgery. Br J Anaesth. 2007;98(4):434–41.
15. Katz ES, Tunick PA, Rusinek H, Ribakove G, Spencer FC, Kronzon I. Protruding aortic atheromas predict stroke risk in elderly patients undergoing cardiopulmonary bypass: experience with intraoperative transesophageal echocardiography. J Am Coll Cardiol. 1992;20(1):70–7.
16. Mussa FF, Horton JD, Moridzadeh, et al. Acute aortic dissection and intramural hematoma: a systematic review. JAMA. 2016;316(7):754–63.
17. LeFevre ML, US Preventive Services Task Force. Screening for abdominal aortic aneurysm: U.S. preventive services task force recommendation statement. Ann Intern Med. 2014;161(4):281–90.
18. Svensjo S, Bjorck M, Wanhainen A. Update on screening for abdominal aortic aneurysm: a topical review. Eur J Vasc Endovasc Surg. 2014;48(6):659–67.
19. Cosford PA, Leng GC. Screening for abdominal aortic aneurysm. Cochrane Database Syst Rev. 2007;2:CD002945.
20. Rubenthaler J, Reiser M, Clevert DA. Diagnostic vascular ultrasound with the help of color Doppler and contrast-enhanced ultrasonography. Ultrasonography. 2016;35(4):289–301.
21. Royse AG, Royse CF. Epiaortic ultrasound assessment of the aorta in cardiac surgery. Best Pract Res Clin Anaesthesiol. 2009;23(3):335–41.
22. Jansen Klomp WW, Brandon Bravo Bruinsma GJ, van't Hof AW, Grandjean JG, Nierich AP. Imaging techniques for diagnosis of thoracic aortic atherosclerosis. Int J Vasc Med. 2016;2016:4726094.
23. de Cilis E, Dachille A, Giardinelli F, Acquaviva T, Bortone AS. Accuracy of intravascular ultrasound evaluation for the assess-

ment of native valve measures in patients undergoing TAVI: preliminary results. Surg Technol Int. 2016;XXIX:201–6.
24. Janosi RA, Gorla R, Rogmann K, Kahlert P, Tsagakis K, Dohle DS, et al. Validation of intravascular ultrasound for measurement of aortic diameters: comparison with multi-detector computed tomography. Minim Invasive Ther Allied Technol. 2015;24(5):289–95.
25. Shi Y, Tsai PI, Wall MJ, Gilani R. Intravascular ultrasound enhanced aortic sizing for endovascular treatment of blunt aortic injury. J Trauma Acute Care Surg. 2015;79(5):817–21.
26. Stavropoulos SW, Charagundla SR. Imaging techniques for detection and management of endoleaks after endovascular aortic aneurysm repair. Radiology. 2007;243(3):641–55.
27. Wolak A, et al. Aortic size assessment by noncontrast cardiac computed tomography: Normal limits by age, gender, and body surface area. J Am Coll Cardiol Img. 2008;1(2):200–9.
28. Nagpal P, Khandelwal A, Saboo SS, Bathla G, Steigner ML, Rybicki FJ. Modern imaging techniques: applications in the management of acute aortic pathologies. Postgrad Med J. 2015;91:449–62.
29. Bitar R, Leung G, Perng R, et al. MR pulse sequences: what every radiologist wants to know but is afraid to ask. Radiographics. 2006;26:513–37.
30. Kawel-Boehm N, Maceira A, Valsangiacomo-Buechel ER, et al. Normal values for cardiovascular magnetic resonance in adults and children. J Cardiovasc Magn Reson. 2015;17:29.
31. Davis A, Lewandowski A, Holloway C, et al. Observational study of regional aortic size referenced to body size: production of a cardiovascular magnetic resonance nomogram. J Cardiovasc Magn Reson. 2014;16:9.
32. Eikendal AL, Bots ML, Haaring C, et al. Reference values for cardiac and aortic magnetic resonance imaging in healthy, young Caucasian adults. PLoS One. 2016;11(10):e0164480.